2023 62nd IEEE Conference on Decision and Control (CDC)
December 13-15, 2023. Marina Bay Sands, Singapore

Human Multi-agent Interaction for Optical Manipulation of Micro-objects

Gulam Dastagir Khan*, Quang Minh Ta* and Chien Chern Cheah

Abstract— **Automated optical manipulation systems are faster and more precise than humans, but less adaptable to uncertainty. A collaborative approach between humans and automated agents can leverage both human reasoning skills and the precision of automated systems. This paper describes a human multi-agent interaction approach for dealing with unexpected events during optical manipulation. The proposed multi-mode control system improves the flexibility and dependability of existing systems, allowing for stable interaction between humans and machines. Experimental validation confirms the effectiveness of the proposed method.**

I. Introduction

Micro-manipulation is the precise handling and manipulation of micro or nanoscale objects using specialized techniques. Optical tweezers use laser beams for non-invasive and precise control of microscopic particles and biological entities [1]–[3], and have applications in many fields for studying micro-scale phenomena [4]–[6].

Optical micro-manipulation has evolved significantly since its inception. Initially, optical traps were manually steered in the specimen plane [7]–[10], but this approach was imprecise, inaccurate, and unreliable. To address these challenges, automated techniques were developed, and several control methods have been proposed. For instance, Ibanez *et al.* [11] developed a simple control approach for handling microscopic objects. Similarly, Banerjee *et al.* [12] described planning approaches for automated micro-manipulation operations, and Cheah *et al.* [13] proposed a basic setpoint control approach for a biological cell trapped by a laser beam. Xie *et al.* [14] proposed a system based on holographic optical tweezers (HOT) for rotational and translational control of a trapped cell. However, these approaches only allowed manipulation of a single cell or micro-object at a time.

Multiple independent traps significantly contribute to laser tweezers' use in drug delivery, cell sorting, and separation [15]–[17]. Various approaches have been proposed for automated transportation of cells, including robot-tweezer manipulation [15], indirect manipulation planning [16], and cooperative mobile manipulation [17]. Stochastic control approaches for manipulating multiple micro-objects were also investigated [18], [19].

In time-pressed, dynamic environments, automated multi-agent systems outperform humans, but they struggle with unexpected circumstances. Human operators can help these systems by providing knowledge-based reasoning, resulting in optimal precision and reasoning capabilities. This collaboration between humans and automated systems has been achieved through physical robotic manipulation. It is, however, difficult to replicate such collaboration in the micro-world. Ta *et al.* [20] introduced a primary approach to human-machine interaction control in optical cell manipulation. However, this approach has a limited scope of human participation. It allows humans to interact with the system solely for obstacle detection and guiding the manipulation system around obstacles. Complex micro-manipulation tasks necessitate more extensive human control or oversight of the automation system.

Our study presents a novel approach that formulates a stable human-triggering method for situations where the automated system is inadequate. In these scenarios, human intervention becomes necessary to support the automated process without any disruptions. This intervention, also referred to as an "event," ensures stable interaction between humans and the automated system. Furthermore, our proposed method enables human decision-making to identify event-triggering scenarios without relying on specific conditions. The fully automated micro-manipulation systems presented in [17], [19], [21] have certain limitations that hinder their ability to execute complex micro-manipulation tasks effectively in unexpected scenarios. These limitations include fixed tasks, such as fixed formations and a fixed number of micro-objects that cannot be modified in response to changes in the situation. Moreover, these approaches are restricted by limited sensing capabilities, which rely solely on a camera with a restricted field of view (FOV), making it difficult to respond to changes. Finally, any changes to the setup require the system to be restarted. The proposed human-triggering in this paper addresses these limitations by increasing the flexibility and dynamism of human intervention and interaction with the system. This new approach enhances the efficiency and efficacy of the micro-manipulation process by allowing for human oversight and intervention when necessary, resulting in coordinated actions that achieve successful micro-manipulation while maintaining stable human-machine interaction in unexpected scenarios.

This paper investigates the challenges of two intricate micro-manipulation scenarios in a limited field of view:

G. D. Khan is with the Dept. of Electrical and Computer Engineering, Sultan Qaboos University (SQU), Muscat, Oman. g.khan1@squ.edu.om. G. D. Khan is the corresponding author.

Q. M. Ta is with the Coordinated Science Lab, University of Illinois at Urbana-Champaign (UIUC), USA. quangminh2702@gmail.com.

C. C. Cheah is with the School of Electrical & Electronic Engineering, Nanyang Technological University, Singapore. ecccheah@ntu.edu.sg.

*These authors contributed equally to the work and are therefore co-first authors.

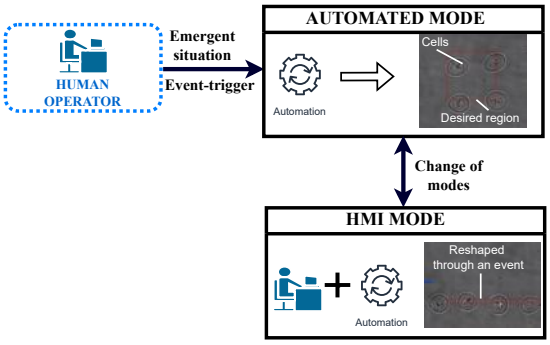

Fig. 1: The proposed methodology for human multi-agent control in optical manipulation of micro-objects.

adding/removing cells from a target cluster and reshaping its formation for safe navigation through narrow passages. This paper presents the design of the controller and a stability study of the closed-loop controller. Eventually, the effectiveness of the proposed method is experimentally validated.

II. Human Multi-Mode Interaction Control

A. Problem statement

Human intervention becomes crucial when the automated system is inadequate. This intervention, referred to as an "event," supports and stabilizes the automated process without disruptions. Human decision-making plays a key role in identifying event-triggering scenarios without specific conditions. Hence, the goal is to ensure stable human intervention to assist the automated process in uncertain or changing conditions. Figure 1 shows how human multi-agent control is used. The automated task operates continuously, except during emergencies, when humans trigger an event and shift the system to human multi-agent mode.

When undertaking micro-manipulation tasks, it is often beneficial to have a plan in place to explicitly define a range of event-triggering conditions or scenarios before commencing the task. This approach can help improve efficiency by enabling a structured process to guide the manipulation process. In the context of the two micro-manipulation scenarios explored in this study, a number of events were identified that could be defined to help facilitate the task. These events were carefully selected to ensure that they effectively addressed specific challenges that might arise during the manipulation process. By defining these events ahead of time, operators are able to work more effectively and efficiently, with a greater degree of control over the process.

The proposed multi-agent manipulation system incorporates several events that facilitate the smooth and efficient manipulation of agents in a formation. Firstly, the system defines an event that activates a new laser tweezer to trap and add a cell of interest into the target cluster of multi-agents. Similarly, to release an agent or cell from the formation, the system defines another event that deactivates the existing laser beam. These events allow the system to add or remove an agent or cell from the formation as required. Secondly, to ensure smooth scaling of the desired region, the system defines an event that varies the region's shape and size while maintaining a minimum distance between the agents or cells in the formation. This enables collision-free manipulation of the agents and allows the system to adapt to changes in the desired region shape. Thirdly, to assist the multi-agent system with effective obstacles avoidance, the system defines an event that enables the provision of reference regions. This event generates the reference positions provided by humans and smoothly pulls the manipulated agents or cells towards the desired location.

We propose a human multi-agent interaction control method based on region-based control [22]. A desired dynamic region for the cluster of cells can be specified as [22]:

$$a(\Delta \boldsymbol{X}_i) = \begin{bmatrix} a_1(\Delta \boldsymbol{X}_i) & a_2(\Delta \boldsymbol{X}_i) & \cdots & a_m(\Delta \boldsymbol{X}_i) \end{bmatrix}^T \leq 0 \tag{1}$$

where $$\Delta \boldsymbol{X}_i = [\Delta X_{i1}, \Delta X_{i2}]^T = \mathbf{T}_v^{-1} \Delta \boldsymbol{x}_i, \tag{2}$$

$\Delta \boldsymbol{x}_i = (\boldsymbol{x}_i - \boldsymbol{x}_0)$, $\boldsymbol{x}_i = [x_{i1}, x_{i2}]^T \in \mathcal{R}^2$ is the position of the trapped agent or cell i. The matrix $\mathbf{T}_v$ is a differentiable and invertible scaling matrix that varies with time, and $\boldsymbol{x}_0 = [x_{01}, x_{02}]^T \in \mathcal{R}^2$ denotes the region's reference point. The set $a(\Delta \boldsymbol{X}_i)$ represents all scalar functions $a_l(\Delta \boldsymbol{X}_i)$, where $l = 1, 2, \cdots, m$, with m being the total number of sub-regions. All $a_l(\Delta \boldsymbol{X}_i)$ have continuous partial derivatives. It is important to note that the desired region $a(\Delta \boldsymbol{X}_i)$ is the intersection of all sub-regions $a_l(\Delta \boldsymbol{X}_i)$, where $l = 1, 2, \cdots, m$. For instance, a desired region with a circular shape is achieved by defining:

$$a(\Delta \boldsymbol{X}_i) = \{\Delta X_{i1}\}^2 + \{\Delta X_{i2}\}^2 - R^2 \leq 0 \tag{3}$$

with R being the radius of the desired region. R must be set with respect to the number of cells being manipulated. If the number of cells are large, then the region is enlarged accordingly to contain all the cells. Here is another example of a rectangular region, defined by a set of inequalities:

$$\begin{aligned} a_1(\Delta \boldsymbol{X}_i) &= \{\Delta X_{i1}\}^2 - a^2 \leq 0, \\ a_2(\Delta \boldsymbol{X}_i) &= \{\Delta X_{i2}\}^2 - b^2 \leq 0 \end{aligned} \tag{4}$$

with a and b being the length and the width of the desired rectangular region. Note that the region's size can be varied or scaled by the time-varying scaling matrix $\mathbf{T}_v$ in $2D$, which can be simply given by:

$$\mathbf{T}_v = \begin{bmatrix} T_{vx}(t) & 0 \\ 0 & T_{vy}(t) \end{bmatrix}. \tag{5}$$

with scaling factors $T_{vx}(t)$ and $T_{vy}(t)$. Therefore, the desired region of circle in (3), for example, can thus be scaled up/down by a following scaling factor

$$\mathbf{T}_v(t) = \begin{cases} \mathbf{T}_v(t_{k-1}) & t \leq t_k \\ \mathbf{T}_v(t_{k-1}) + \Delta \mathbf{T} \Big(\frac{6}{\Delta t^5}(t - t_k)^5 & \\ -\frac{15}{\Delta t^4}(t - t_k)^4 & \\ +\frac{10}{\Delta t^3}(t - t_k)^3 \Big) & t_k < t < t_k + \Delta t \\ \mathbf{T}_v(t_{k-1}) + \Delta \mathbf{T} & t > t_k + \Delta t \end{cases} \tag{6}$$

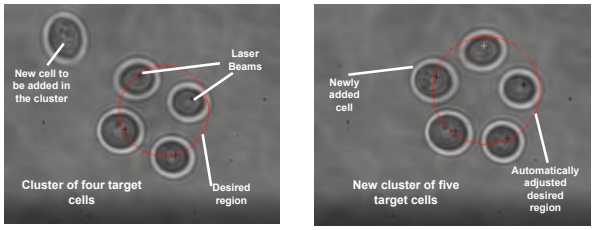

Fig. 2: An illustration of scaling up the desired circular region in $2D$ space to add a new cell.

where $\mathbf{T}_v(t_{k-1}) > 0$ is the current (constant) scale before a new event is triggered at $t = t_k$, Δt is a predefined transition time of the event and all other events or triggering are disabled during this period. Figure 2 shows that the desired reference region, represented by a circle, can be scaled up with just one event by simultaneously modifying T_{vx} and T_{vy} using (6). When reshaping a square or rectangle region, it's important to adjust only one axis at a time to ensure a smooth and accurate transformation. In Figure 1, the original square region is transformed into a rectangle by adjusting T_{vx} and T_{vy} sequentially. This requires executing the scaling event twice, once for the x-axis variation and once for the y-axis variation. To aid agents/cells in obstacle avoidance, the human triggers a stop event causing the desired region and its velocity $\dot{\boldsymbol{x}}_0$ to smoothly transition to zero. Reference position is then provided by the human and reference velocity is estimated via differentiation.

Each event is triggered by a human at a specific time t_k, but a new event cannot be triggered until the previous one has completed. This prevents the problem of Zeno behavior, which is an infinite number of events within a finite time interval, from occurring.

B. Theoretical analysis

This subsection proposes a stable human-triggering strategy for complex micro-manipulation scenarios, enabling human operators to interact with a stochastic cell manipulation system through event initiation. The strategy is particularly useful for tasks such as adding or removing cells from a cluster and reshaping its formation for collision-free passage through a narrow passage.

The stochastic motion process of cells in the presence of the laser beam's trapping force is expressed as [19]:

$$\boldsymbol{M_i}\ddot{\boldsymbol{x}}_i = -\boldsymbol{B}_i\dot{\boldsymbol{x}}_i + \boldsymbol{k}_i(\boldsymbol{q}_i - \boldsymbol{x}_i) + \boldsymbol{F}_i \tag{7}$$

where $\boldsymbol{M}_i = \mathrm{diag}\{\mathrm{m_i}, \mathrm{m_i}\} \in \mathcal{R}^{2\times 2}$ and $\boldsymbol{B}_i = \mathrm{diag}\{\mathrm{b_{i1}}, \mathrm{b_{i2}}\} \in \mathcal{R}^{2\times 2}$ respectively represent the inertia and damping matrices of the cell i. The stiffness of the i^{th} optical tweezer is represented by $\boldsymbol{k}_i = \mathrm{diag}\{\mathrm{k_{i1}}, \mathrm{k_{i2}}\} \in \mathcal{R}^{2\times 2}$, $\boldsymbol{q}_i = (q_{i1}, q_{i2})^T \in \mathcal{R}^2$ denotes the position of the corresponding laser beam that traps and manipulates the agent i. The force $\boldsymbol{F}_i = \mathrm{diag}\{\sqrt{2\mathrm{k_B}\bar{T}\mathrm{b_{i1}}}, \sqrt{2\mathrm{k_B}\bar{T}\mathrm{b_{i2}}}\}(\zeta_{i1}, \zeta_{i2})^{\mathrm{T}} \in \mathcal{R}^2$ is the two-dimensional Brownian force where k_B is the Boltzmann's constant, $\bar{T}$ is the absolute temperature, and $\zeta_{ip} = \frac{dW_{ip}}{dt}$, $p = 1, 2$, are stochastic Gaussian white noises.

To begin, we define a potential energy function that manipulates cell i towards a target region as [21]:

$$T_{P_i} = \sum_{l=1}^{m} \frac{\delta}{\beta}\{\max[0, a_l(\Delta \boldsymbol{X}_i)]\}^{\beta} \tag{8}$$

where δ, $\beta > 0$ and $\beta > 2$, ensuring that T_{P_i} is twice differentiable. A control force for manipulating the cells toward the target region can be designed as $\Delta\boldsymbol{\xi}_{T_i} = \frac{\partial T_{P_i}}{\partial(\Delta \boldsymbol{X}_i)}$:

$$\Delta\boldsymbol{\xi}_{T_i} = \sum_{l=1}^{m} \delta[\max[0, a_l(\Delta \boldsymbol{X}_i)]]^{\beta-1}\Big[\frac{\partial a_l(\Delta \boldsymbol{X}_i)}{\partial(\Delta \boldsymbol{X}_i)}\Big]^T. \tag{9}$$

When cells are outside the target region, the force $\Delta\boldsymbol{\xi}_{T_i}$ from (9) pulls the cells toward the region, and when the cells are inside the region $\Delta\boldsymbol{\xi}_{T_i} = 0$.

In order to ensure collision-free transportation of cells within the target cluster of multi-agent, a potential energy function has been proposed for maintaining the minimum distance between cells. This potential energy function is formulated as follows [21]:

$$C_{iq} = \sum_{q\in\mathcal{N}_i} \frac{\sigma_{iq}}{\beta}\{\max[0, h_{iq}(\Delta \boldsymbol{X}_{iq})]^{\beta}\} \tag{10}$$

where $\mathcal{N}_i$ represents the set of neighbor cells around cell i within the target cluster of multi-agent, and σ_{iq} are positive constants. The inequality $h_{iq}(\Delta \boldsymbol{X}_{iq}) = r^2 - |\mathbf{T}_v^{-1}\Delta \boldsymbol{x}_{iq}|^2 \leq 0$ defines the minimum distance between cells in the target cluster, where $\Delta \boldsymbol{x}_{iq} = \boldsymbol{x}_i - \boldsymbol{x}_q$ represents the distance between neighboring cells i and q in the target cell cluster. It is important to note that the minimum distance between cells varies with time based on the transformation matrix $\mathbf{T}_v$.

A control force for maintaining a minimum distance between cells in the target cluster is then defined as $\Delta\boldsymbol{\eta}_{iq} = \frac{\partial C_{iq}}{\partial(\Delta \boldsymbol{X}_{iq})}$:

$$\Delta\boldsymbol{\eta}_{iq} = \sum_{q\in\mathcal{N}_i} \sigma_{iq}\{\max[0, h_{iq}(\Delta \boldsymbol{X}_{iq})]\}^{\beta-1} \times \Big[\frac{\partial h_{iq}(\Delta \boldsymbol{X}_{iq})}{\partial(\Delta \boldsymbol{X}_{iq})}\Big]^T. \tag{11}$$

When the distance between two neighboring cells i and q is too close, that is $\|\mathbf{T}_v^{-1}\Delta \boldsymbol{x}_{iq}\| < r$, the resultant force $\Delta\boldsymbol{\eta}_{iq}$ is activated to push cell i away from cell q. When a minimum distance is maintained between neighboring cells, that is $\|\mathbf{T}_v^{-1}\Delta \boldsymbol{x}_{iq}\| \geq r$, the resultant force $\Delta\boldsymbol{\eta}_{iq} = \mathbf{0}$.

The approach involves manipulating the control forces defined in (9) and (11) at triggering instant to achieve complex micro-manipulation scenarios. To add a new cell i to an existing target cluster, a sequence of events is triggered. The first event manipulates the control force $\Delta\boldsymbol{\eta}_{iq}$ in (11) to resize the desired region using the time-varying scaling matrix $\mathbf{T}_v$ in (5). Then, another event is triggered to activate a new laser tweezer that uses the control force $\Delta\boldsymbol{\xi}_{T_i}$ in (9) to trap and drive the new cell i towards the desired region. To release an agent or cell from the formation, a third event is defined to deactivate the existing laser beam. Finally, the fourth event adjusts the control force $\Delta\boldsymbol{\eta}_{iq}$ in (11) to change the desired region shape accordingly. To achieve

smooth multi-agent passage maneuvering, a sequence of events is initiated to adjust the size and shape of the desired region, with the control force $\Delta\boldsymbol{\eta}_{iq}$ in (11) being manipulated accordingly. Furthermore, an event is triggered to generate reference positions from humans to aid in obstacle avoidance, pulling the agents or cells towards the desired location in a smooth manner.

Let $\Delta\boldsymbol{\xi}_i = \alpha\Delta\boldsymbol{\xi}_{T_i} + \gamma\Delta\boldsymbol{\eta}_{iq}$, where α, $\gamma > 0$, be general control force for the proposed interaction control system. Firstly, we define the reference velocity as:

$$\dot{\boldsymbol{x}}_{ri} = \dot{\boldsymbol{x}}_0 - \boldsymbol{T}_v\frac{d}{dt}(\boldsymbol{T}_v^{-1})\Delta\boldsymbol{x}_i - \boldsymbol{T}_v\Delta\boldsymbol{\xi}_i. \tag{12}$$

A sliding vector is introduced for each controlled agent, as follows:

$$\begin{aligned}\boldsymbol{s}_i = \dot{\boldsymbol{x}}_i - \dot{\boldsymbol{x}}_{ri} &= \Delta\dot{\boldsymbol{x}}_i + \boldsymbol{T}_v\frac{d}{dt}(\boldsymbol{T}_v^{-1})\Delta\boldsymbol{x}_i + \boldsymbol{T}_v\Delta\boldsymbol{\xi}_i \\ &= \boldsymbol{T}_v(\Delta\dot{\boldsymbol{X}}_i + \Delta\boldsymbol{\xi}_i).\end{aligned} \tag{13}$$

Equation (7) can be rewritten as

$$\ddot{\boldsymbol{x}}_i = -\boldsymbol{M}_{\boldsymbol{i}}^{-1}\boldsymbol{B}_i\dot{\boldsymbol{x}}_i + \boldsymbol{M}_{\boldsymbol{i}}^{-1}\boldsymbol{k}_i(\boldsymbol{q}_i - \boldsymbol{x}_i) + \boldsymbol{M}_{\boldsymbol{i}}^{-1}\boldsymbol{F}_i. \tag{14}$$

With the aid of the sliding vectors as specified in (13), it is possible to rewrite (14) as follows

$$\begin{aligned}\dot{\boldsymbol{s}}_i + \boldsymbol{D}_i\boldsymbol{s}_i + \ddot{\boldsymbol{x}}_{ri} + \boldsymbol{Y}(\dot{\boldsymbol{x}}_{ri})\boldsymbol{\phi}_i + \boldsymbol{M}_i^{-1}\boldsymbol{k}_i\boldsymbol{x}_i - \boldsymbol{M}_i^{-1}\mathbf{F}_i \\ = \boldsymbol{M}_i^{-1}\boldsymbol{k}_i\boldsymbol{q}_i\end{aligned} \tag{15}$$

where $\boldsymbol{D}_i = \boldsymbol{M}_i^{-1}\boldsymbol{B}_i$, $\boldsymbol{D}_i\dot{\boldsymbol{x}}_{ri} = \boldsymbol{Y}(\dot{\boldsymbol{x}}_{ri})\boldsymbol{\phi}_i$ with vectors of unknown parameters $\boldsymbol{\phi}_i$ and known regressor matrices $\boldsymbol{Y}(\dot{\boldsymbol{x}}_{ri})$.

We propose a controller for the human multi-agent interaction system as:

$$\boldsymbol{q}_i = \boldsymbol{x}_i - \boldsymbol{K}_i\boldsymbol{s}_i + \hat{\boldsymbol{\mu}}_i^{-1}\ddot{\boldsymbol{x}}_{ri} + \hat{\boldsymbol{\mu}}_i^{-1}\boldsymbol{Y}(\dot{\boldsymbol{x}}_{ri})\hat{\boldsymbol{\phi}}_i + \hat{\boldsymbol{\mu}}_i^{-1}\boldsymbol{Y}_\mu(\boldsymbol{\omega}_i)\hat{\boldsymbol{\theta}}_i, \tag{16}$$

where $\boldsymbol{K}_i \in \mathbf{R}^{2\times2}$ are positive-definite and diagonal gain matrices, $\hat{\boldsymbol{\mu}}_i$ are estimated diagonal matrices of the diagonal matrices $\boldsymbol{\mu}_i = \boldsymbol{M}_i^{-1}\boldsymbol{k}_i$. The terms $\boldsymbol{Y}_\mu(\boldsymbol{\omega}_i)\hat{\boldsymbol{\theta}}_i$ are utilized to compensate for the uncertainties of parameters $\boldsymbol{\mu}_i$ in which $\boldsymbol{Y}_\mu(\boldsymbol{\omega}_i) = \mathrm{diag}\{\omega_{i1}, \omega_{i2}\}$ is a known regressor matrices with $\boldsymbol{\omega}_i = \boldsymbol{Y}(\dot{\boldsymbol{x}}_{ri})\hat{\boldsymbol{\phi}}_i + \ddot{\boldsymbol{x}}_{ri}$. The unknown parameters $\hat{\boldsymbol{\theta}}_i$ are estimations of $\boldsymbol{\theta}_i$ which are updated by

$$\dot{\hat{\boldsymbol{\theta}}}_i = -\tau_\theta\hat{\boldsymbol{\theta}}_i - \boldsymbol{L}_\theta\boldsymbol{Y}_\mu^T(\boldsymbol{\omega}_i)\boldsymbol{s}_i, \tag{17}$$

with constant $\tau_\theta > 0$ and matrix $\boldsymbol{L}_\theta \in \mathcal{R}^{2\times2}$ diagonal and positive definite. In (16), adaptive terms $\boldsymbol{Y}(\dot{\boldsymbol{x}}_{ri})\hat{\boldsymbol{\phi}}_i$ are used to account for uncertainties in the dynamics of the manipulated cell, and $\hat{\boldsymbol{\phi}}_i$ are estimations of $\boldsymbol{\phi}_i$ which are updated by

$$\dot{\hat{\boldsymbol{\phi}}}_i = -\kappa_\phi\hat{\boldsymbol{\phi}}_i - \boldsymbol{L}_\phi\boldsymbol{Y}^T(\dot{\boldsymbol{x}}_{ri})\boldsymbol{s}_i, \tag{18}$$

with constant $\kappa_\phi > 0$ and matrix $\boldsymbol{L}_\phi \in \mathcal{R}^{2\times2}$ diagonal and positive definite. By substituting (16) into (15) and after simplification, we can derive the dynamic equations of the closed-loop system as follows:

$$\begin{aligned}\dot{\boldsymbol{s}}_i + (\boldsymbol{D}_i + \boldsymbol{\mu}_i\boldsymbol{K}_i)\boldsymbol{s}_i + \boldsymbol{Y}(\dot{\boldsymbol{x}}_{ri})\Delta\boldsymbol{\phi}_i + \boldsymbol{Y}_\mu(\boldsymbol{\omega}_i)\Delta\bar{\boldsymbol{\theta}}_i \\ - \boldsymbol{M}_i^{-1}\boldsymbol{F}_i = 0\end{aligned} \tag{19}$$

with $\Delta\boldsymbol{\phi}_i = \boldsymbol{\phi}_i - \hat{\boldsymbol{\phi}}_i$, $\Delta\bar{\boldsymbol{\theta}}_i = \bar{\boldsymbol{\theta}}_i - \boldsymbol{\mu}_i\hat{\boldsymbol{\mu}}_i^{-1}\hat{\boldsymbol{\theta}}_i$ and vectors of unknown parameters $\bar{\boldsymbol{\theta}}_i = (\boldsymbol{I}_2 - \boldsymbol{\mu}_i\hat{\boldsymbol{\mu}}_i^{-1})(1,1)^T \in \mathcal{R}^2$. From (17), (18), and (19), the closed-loop equations can be rewritten in the form of a stochastic differential equation as:

$$d\boldsymbol{\Upsilon}_i = \boldsymbol{\Psi}_i dt + \boldsymbol{\Theta}_i d\boldsymbol{\Gamma}_i, \tag{20}$$

where $\boldsymbol{\Upsilon}_i = (\boldsymbol{s}_i^T, \Delta\boldsymbol{\phi}_i^T, \Delta\bar{\boldsymbol{\theta}}_i^T)^T$, $\boldsymbol{\Psi}_i = (\Psi_i^1, \Psi_i^2, \Psi_i^3)^T$ with $\Psi_i^1 = -(\boldsymbol{D}_i + \boldsymbol{\mu}_i\boldsymbol{K}_i)\boldsymbol{s}_i - \boldsymbol{Y}(\dot{\boldsymbol{x}}_{ri})\Delta\boldsymbol{\phi}_i - \boldsymbol{Y}_\mu(\boldsymbol{\omega}_i)\Delta\bar{\boldsymbol{\theta}}_i$, $\Psi_i^2 = \kappa_\phi\hat{\boldsymbol{\phi}}_{\boldsymbol{i}} + \boldsymbol{L}_\phi\boldsymbol{Y}^T(\dot{\boldsymbol{x}}_{ri})\boldsymbol{s}_i$ and $\Psi_i^3 = \boldsymbol{\mu}_i\hat{\boldsymbol{\mu}}_i^{-1}(\tau_\theta\hat{\boldsymbol{\theta}}_{\boldsymbol{i}} + \boldsymbol{L}_\theta\boldsymbol{Y}_\mu^T(\boldsymbol{\omega}_i)\boldsymbol{s}_i)$. $\boldsymbol{\Theta}_i = \mathrm{diag}\{\boldsymbol{\Sigma}_i, \mathbf{0}, \mathbf{0}\}$ and $\boldsymbol{\Gamma}_i = (\boldsymbol{W}_i^T, \mathbf{0}^T, \mathbf{0}^T)^T$ where $\mathbf{0} \in \mathcal{R}^2$ is the null vector, $\boldsymbol{\Sigma}_{\boldsymbol{i}} = \mathrm{diag}\{\sqrt{\frac{2k_BTb_{i1}}{m_i^2}}, \sqrt{\frac{2k_BTb_{i2}}{m_i^2}}\}$ and $\boldsymbol{W}_i = [W_{i1}, W_{i2}]^T$ are Wiener processes.

To prove the stability of the closed-loop control system described in (20) consider a Lyapunov-like candidate function $V(t)$ as

$$\begin{aligned}V(t) = \frac{1}{2}\sum_{i=1}^{N}\boldsymbol{s}_i^T\boldsymbol{s}_i + \frac{1}{2}\sum_{i=1}^{N}\Delta\boldsymbol{\phi}_i^T\boldsymbol{L}_\phi^{-1}\Delta\boldsymbol{\phi}_i \\ + \frac{1}{2}\sum_{i=1}^{N}\Delta\bar{\boldsymbol{\theta}}_i^T\hat{\boldsymbol{\mu}}_i\boldsymbol{\mu}_i^{-1}\boldsymbol{L}_\theta^{-1}\Delta\bar{\boldsymbol{\theta}}_i.\end{aligned} \tag{21}$$

The differential generator of $V(t)$, denoted as $\mathcal{D}[V(t)]$, is given as:

$$\begin{aligned}\mathcal{D}[V(t)] = \sum_{i=1}^{N}\{\frac{\partial V(t)}{\partial\boldsymbol{s}_i}\Psi_i^1 + \frac{\partial V(t)}{\partial\Delta\boldsymbol{\phi}_i}\Psi_i^2 + \frac{\partial V(t)}{\partial\Delta\bar{\boldsymbol{\theta}}_i}\Psi_i^3 \\ + \frac{1}{2}tr[\mathrm{diag}(\boldsymbol{\Sigma}_i^T\boldsymbol{\Sigma}_i, \mathbf{0}, \mathbf{0})]\}\end{aligned} \tag{22}$$

with $tr[\cdot]$ representing the trace of a matrix. Using (20) and (21) into (22) and simplifying yields

$$\begin{aligned}\mathcal{D}[V(t)] = \sum_{i=1}^{N}\Big\{ - \boldsymbol{s}_i^T(\boldsymbol{D}_i + \boldsymbol{\mu}_i\boldsymbol{K}_i)\boldsymbol{s}_i + \kappa_\phi\Delta\boldsymbol{\phi}_i^T\boldsymbol{L}_\phi^{-1}\hat{\boldsymbol{\phi}}_i \\ + \tau_\theta\Delta\bar{\boldsymbol{\theta}}_i^T\boldsymbol{L}_\theta^{-1}\hat{\boldsymbol{\theta}}_i + (\frac{k_BTb_{i1}}{m_i^2}, \frac{k_BTb_{i2}}{m_i^2})\Big\}.\end{aligned} \tag{23}$$

The objective is to prove the following inequality:

$$\mathcal{D}[V(t)] \leq -2\varphi V(t) + \upsilon \tag{24}$$

with positive constants φ and υ. It is worth noting that there exists positive constants φ_s, φ_ϕ and φ_θ such that the following three inequalities

$$-\sum_{i=1}^{N}\boldsymbol{s}_i^T(\boldsymbol{D}_i + \boldsymbol{\mu}_i\boldsymbol{K}_i)\boldsymbol{s}_i \leq -\sum_{i=1}^{N}\varphi_s\boldsymbol{s}_i^T\boldsymbol{s}_i,$$

$$\sum_{i=1}^{N}\kappa_\phi\Delta\boldsymbol{\phi}_i^T\boldsymbol{L}_\phi^{-1}\hat{\boldsymbol{\phi}}_i \leq \sum_{i=1}^{N}\{\kappa_\phi\frac{l_\phi^{-1}}{2}\|\boldsymbol{\phi}_i\|^2 - \varphi_\phi\Delta\boldsymbol{\phi}_i^T\boldsymbol{L}_\phi^{-1}\Delta\boldsymbol{\phi}_i\}$$

with $l_\phi > 0$ and

$$\begin{aligned}\sum_{i=1}^{N}\tau_\theta\Delta\bar{\boldsymbol{\theta}}_i^T\boldsymbol{L}_\theta^{-1}\hat{\boldsymbol{\theta}}_i \leq \sum_{i=1}^{N}\tau_\theta\frac{l_\theta^{-1}}{2\mu}\|\bar{\boldsymbol{\theta}}_i\|^2 \\ - \sum_{i=1}^{N}\varphi_\theta\Delta\bar{\boldsymbol{\theta}}_i^T\hat{\boldsymbol{\mu}}_i\boldsymbol{\mu}_i^{-1}\boldsymbol{L}_\theta^{-1}\Delta\bar{\boldsymbol{\theta}}_i\end{aligned}$$

with $l_\theta, \mu > 0$ hold. Then it can be proven that their exists φ satisfying $\varphi = \min\{\varphi_s, \varphi_\phi, \varphi_\theta\}$ and $\upsilon = \sum_{i=1}^{N}\{\kappa_\phi \frac{l_\phi^{-1}}{2}\|\boldsymbol{\phi}_i\|^2 + \tau_\theta \frac{l_\theta^{-1}}{2\mu}\|\bar{\boldsymbol{\theta}}_i\|^2 + (\frac{k_B T b_{i1}}{m_i^2}, \frac{k_B T b_{i2}}{m_i^2})\}$ such that for all $t \geq 0$ [18]

$$\mathcal{M}[V(t)] \leq \frac{\upsilon}{2\varphi} + \left(V(0) - \frac{\upsilon}{2\varphi}\right)^{+} e^{-2\varphi t} \tag{25}$$

with $\mathcal{M}[V(t)]$ denoting the expectation of $V(t)$, and $[\cdot]^+ = \max(\cdot, 0)$. From equation (25), it can be concluded that $\mathcal{M}[V(t)]$ is bounded. Consequently, $\boldsymbol{s}_i$, $\Delta\boldsymbol{\phi}_i$, and $\Delta\bar{\boldsymbol{\theta}}i$ for $i = 1, \cdots, N$ are also bounded. Furthermore, since $\Delta\boldsymbol{\xi}i$, $\Delta\boldsymbol{\xi}_{T_i}$, and $\Delta\boldsymbol{\eta}_{iq}$ are bounded, the boundedness of $\boldsymbol{s}_i$, as defined in (13), guarantees the boundedness of $\Delta\dot{\boldsymbol{X}}_i$ for $i = 1, \cdots, n$. The next statement presents the following theorem:

Theorem 1. *The proposed controller (16), along with update laws (17) and (18), ensures the stability of human multi-agent interaction during complex optical manipulation of cells, even in the presence of stochastic perturbations.*

III. Experiment

The proposed approach for human multi-agent interaction was implemented on an E3500 optical tweezers system at Nanyang Technological University. The system mainly consists of a device for steering multiple optical traps (Elliot Scientific), an inverted microscope (Nikon, Eclipse TiU), and a CCD camera (Basler, pi640-210gm). The manipulation space for cells under the field of view of the camera is a rectangular area with dimensions of $47.95\mu m \times 36.11\mu m$. The proposed control algorithm that enables human multi-agent interaction was written in National Instrumental LabVIEW so as to control the position of laser beams.

In the following experiments, yeast cells with diameters ranging from 3-5μm were utilized to be the manipulated objects. The cells were immersed into ultra pure water (BioRev, Singapore), and then brought onto the sample plane of the microscope. With the usage a computer mouse, humans were able to interact with the automated control system for optical manipulation of biological cell through a Graphical User Interface (GUI). The following experiments address two scenarios that are commonly required in many biological applications. These are adding cells of interest or removing unwanted cells during manipulation, and manipulating a group of cells through constraint environments.

A. Adding cells of interest or removing unwanted cells

Micro-manipulation poses challenges in identifying cells of interest due to the limited field of view (FOV), necessitating human intervention for positive selection and negative selection or removal of unwanted cells. Ensuring stable human-machine interaction is critical. Figures 3 and 4 show the addition and removal of cells in a target cluster through human intervention. During manipulation process, humans were able to interact with the automated cell manipulation system to either add more cell of interest, or remove unwanted cells. The control parameters were set as $\delta = 1, \beta = 4, \sigma_{iq} = 1, \alpha = 1, \gamma = 1, \boldsymbol{K}_i = diag\{0.025, 0.025\}, \boldsymbol{L}_\theta = 10^{-5}\boldsymbol{I}_2$, and $\boldsymbol{L}_\phi = 0.5 \times 10^{-5} \times \boldsymbol{I}_2$ with $\boldsymbol{I}_2$ being a 2×2 identity matrix.

B. Multi-agent group maneuvering through narrow passage

In dynamic micro-manipulation environments, human intervention may be needed to guide multi-agent clusters through narrow spaces. Figure 5 illustrates a sequence of events used by a human operator to navigate the target cells through an obstacle. In this experiment, a square region specified in (4) was utilized for group manipulation of cell, with $a = b$. The control parameters were set the same as in the previous experiment.

IV. Conclusion

Future work can improve the proposed framework for stable human-multi-agent interaction in optical manipulation of micro-objects, including enhancing its adaptability and robustness, expanding its capabilities, and exploring machine learning algorithms for better decision-making.

References

[1] A. Menciassi, A. Eisinberg, I. Izzo, and P. Dario, "From" macro" to" micro" manipulation: models and experiments," *IEEE/ASME Transactions on mechatronics*, vol. 9, no. 2, pp. 311–320, 2004.

[2] A. Ashkin, J. M. Dziedzic, J. E. Bjorkholm, and S. Chu, "Observation of a single-beam gradient force optical trap for dielectric particles," *Optics letters*, vol. 11, no. 5, pp. 288–290, 1986.

[3] A. Ashkin, K. Schütze, J. Dziedzic, U. Euteneuer, and M. Schliwa, "Force generation of organelle transport measured in vivo by an infrared laser trap," *Nature*, vol. 348, pp. 346–348, 1990.

[4] K. Svoboda and S. M. Block, "Biological applications of optical forces," *Annual review of biophysics and biomolecular structure*, vol. 23, no. 1, pp. 247–285, 1994.

[5] E. Ferrari, V. Emiliani, D. Cojoc, V. Garbin, M. Zahid, C. Durieux, M. Coppey-Moisan, and E. Di Fabrizio, "Biological samples micro-manipulation by means of optical tweezers," *Microelectronic Engineering*, vol. 78, pp. 575–581, 2005.

[6] D. Cojoc, V. Garbin, E. Ferrari, L. Businaro, F. Romanato, and E. Di Fabrizio, "Laser trapping and micro-manipulation using optical vortices," *Microelectronic Engineering*, vol. 78, pp. 125–131, 2005.

[7] M. Nishioka, T. Tanizoe, S. Katsura, and A. Mizuno, "Micro manipulation of cells and dna molecules," *Journal of Electrostatics*, vol. 35, no. 1, pp. 83–91, 1995.

[8] S. B. Smith, Y. Cui, and C. Bustamante, "Optical-trap force transducer that operates by direct measurement of light momentum," in *Methods in enzymology*. Elsevier, 2003, vol. 361, pp. 134–162.

[9] D. G. Grier, "A revolution in optical manipulation," *nature*, vol. 424, no. 6950, pp. 810–816, 2003.

[10] K. C. Neuman and S. M. Block, "Optical trapping," *Review of scientific instruments*, vol. 75, no. 9, pp. 2787–2809, 2004.

[11] C. Aguilar-Ibañez, M. S. Suarez-Castanon, and L. I. Rosas-Soriano, "A simple control scheme for the manipulation of a particle by means of optical tweezers," *International Journal of Robust and Nonlinear Control*, vol. 21, no. 3, pp. 328–337, 2011.

[12] A. G. Banerjee and S. K. Gupta, "Research in automated planning and control for micromanipulation," *IEEE Transactions on automation science and engineering*, vol. 10, no. 3, pp. 485–495, 2013.

[13] C. C. Cheah, X. Li, X. Yan, and D. Sun, "Simple pd control scheme for robotic manipulation of biological cell," *IEEE Transactions on Automatic Control*, vol. 60, no. 5, pp. 1427–1432, 2014.

[14] M. Xie, J. K. Mills, Y. Wang, M. Mahmoodi, and D. Sun, "Automated translational and rotational control of biological cells with a robot-aided optical tweezers manipulation system," *IEEE Transactions on Automation Science and Engineering*, vol. 13, no. 2, pp. 543–551, 2015.

[15] S. Hu and D. Sun, "Automatic transportation of biological cells with a robot-tweezer manipulation system," *The International Journal of Robotics Research*, vol. 30, no. 14, pp. 1681–1694, 2011.

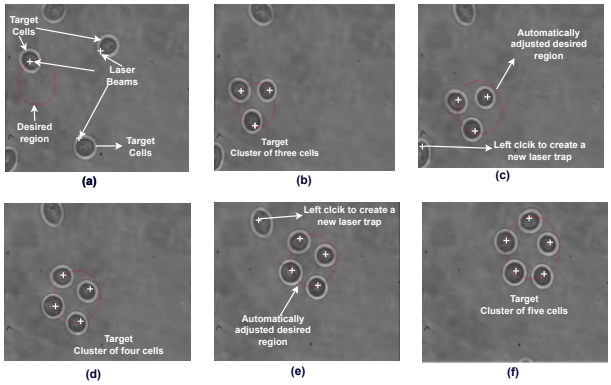

Fig. 3: Adding cells sequentially to a dynamic region. (a). Initial positions. (b). Three cells are manipulated to a dynamic region. (c)-(e). During manipulation, the human operator notices two other cells of interest and plans to add them into the formation. The proposed approach for human multi-agent interaction thus enables the operator to do that in a stable manner without the need to stop the automated process. The operator left-clicks on these cells' positions, and two laser are generated to trap and move these cells accordingly. (f). The cells are manipulated as a whole group while being kept inside the dynamic region.

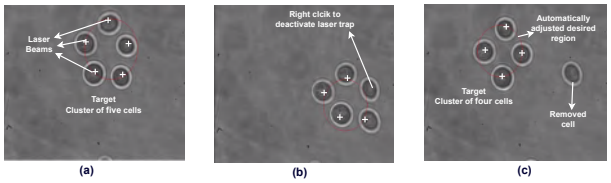

Fig. 4: Removing cell from a dynamic region. (a). A group of cells are manipulated while being kept inside a dynamic region. During manipulation, the human operator notices an unwanted cell and plans to remove it from the formation. The operator right-clicks on that cell's position so as to remove it from the formation in a stable manner (b)-(c).

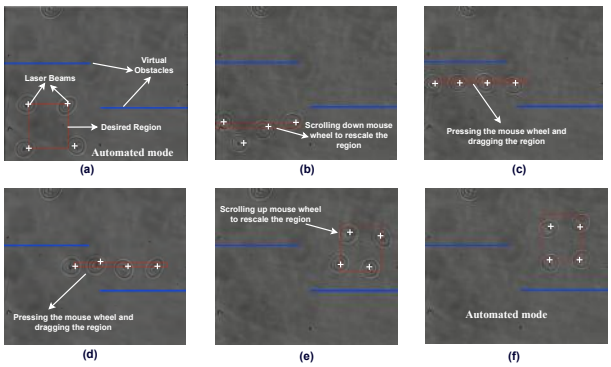

Fig. 5: Multi-agent passage maneuvering. (a) A group of manipulated cells are inside a square dynamic region. (b) While manipulating, obstacles are detected, and the human operator resizes the region into a rectangle by adjusting one axis at a time. (c)-(d) The rectangular region is then smoothly dragged through obstacles using the mouse wheel. (e-f) The region is reshaped back into a square, and cells are manipulated as a group within it using automation.

[16] S. Chowdhury, A. Thakur, P. Švec, C. Wang, W. Losert, and S. K. Gupta, "Automated manipulation of biological cells using gripper formations controlled by optical tweezers," *IEEE Transactions on Automation Science and Engineering*, vol. 11, no. 2, pp. 338–347, 2013.

[17] Q. M. Ta and C. C. Cheah, "Cooperative and mobile manipulation of multiple microscopic objects based on micro-hands and laser-stage control," *Automatica*, vol. 98, pp. 201–214, 2018.

[18] X. Yan, C. C. Cheah, Q. M. Ta, and Q.-C. Pham, "Stochastic dynamic trapping in robotic manipulation of micro-objects using optical tweezers," *IEEE Transactions on Robotics*, vol. 32, no. 3, pp. 499–512, 2016.

[19] Q. M. Ta and C. C. Cheah, "Stochastic control for optical manipulation of multiple microscopic objects," *Automatica*, vol. 89, pp. 52–64, 2018.

[20] ——, "Human–machine interaction control for stochastic cell manipulation systems," *Automatica*, vol. 131, p. 109721, 2021.

[21] C. C. Cheah, Q. M. Ta, and R. Haghighi, "Grasping and manipulation of a micro-particle using multiple optical traps," *Automatica*, vol. 68, pp. 216–227, 2016.

[22] C. C. Cheah, S. P. Hou, and J. J. E. Slotine, "Region-based shape control for a swarm of robots," *Automatica*, vol. 45, no. 10, pp. 2406–2411, 2009.